

# Highly Transparent Alumina Spark Plasma Sintered from Common-Grade Commercial Powder: The Effect of Powder Treatment

Xihai Jin, Lian Gao,<sup>†</sup> and Jing Sun

The State Key Laboratory on High Performance Ceramics and Superfine Microstructure, Shanghai Institute of Ceramics, Shanghai, China 200050

**Transparent alumina were tentatively prepared by spark plasma sintering, using aggregated submicrometer-sized commercial Al<sub>2</sub>O<sub>3</sub> powder. It is found that the pretreatment of the powder in hydrofluoric acid significantly reduces the aggregate size of the powder, suppresses the grain growth, and improves the microstructure homogeneity of the sintered ceramics. The sample sintered from the pretreated powder is highly transparent, while the sample sintered from the untreated powder is translucent at most. The fundamental reasons for this are investigated.**

## I. Introduction

ALUMINA (Al<sub>2</sub>O<sub>3</sub>) shows many interesting properties, such as high strength, high hardness, and excellent corrosive resistance. This makes transparent Al<sub>2</sub>O<sub>3</sub> ceramics a promising candidate for applications as electromagnetic windows, transparent armor, and envelopes of high-pressure metal halide lamps, etc. Traditional transparent Al<sub>2</sub>O<sub>3</sub> ceramics are prepared by sintering in hydrogen gas at temperature generally above 1700°C.<sup>1,2</sup> The high sintering temperature causes extensive grain growth and seriously affects the mechanical strength and hardness of the material. What is more important, the large grain size (> 10 μm) leads to significant light scattering caused by the birefringence of coarse Al<sub>2</sub>O<sub>3</sub> grains.<sup>3</sup> As a result, although traditional transparent Al<sub>2</sub>O<sub>3</sub> ceramics show a high diffuse forward transmission, its in-line transmission is typically below 10%, which makes the material appear translucent rather than transparent. The low strength and in-line transmission pose an almost insurmountable obstacle for application in fields where high transparency and good mechanical properties are required.

Recently, fine-grained transparent Al<sub>2</sub>O<sub>3</sub> ceramics has attracted much attention,<sup>3–10</sup> due to its superior mechanical and optical properties. This material is prepared by hot isostatic pressing or spark plasma sintering at a low temperature around 1150–1300°C. The formation of fine-grained microstructure (< 1 μm) leads to a significant improvement in both the strength and the transparency. It is reported that the strength of the fine-grained transparent Al<sub>2</sub>O<sub>3</sub> is up to 600–800 MPa together with a high in-line transmission up to 60% for visible light.<sup>4,10</sup> In comparison with traditional coarse-grained transparent Al<sub>2</sub>O<sub>3</sub> ceramics, the properties of the fine grained one are much more superior. However, for the preparation of fine-grained transparent Al<sub>2</sub>O<sub>3</sub> ceramics, high-grade α-Al<sub>2</sub>O<sub>3</sub> powder with well-

dispersed nanoparticles and excellent sinterability is needed. The high price and limited sources of such a powder are not beneficial for a large-scale production of the material.

In order to overcome the problem, transparent Al<sub>2</sub>O<sub>3</sub> ceramics were tentatively prepared by spark plasma sintering in the present work, using common grade α-Al<sub>2</sub>O<sub>3</sub> powder that showed a primary particle size in the submicron range and was aggregated as the raw material. We found that highly transparent Al<sub>2</sub>O<sub>3</sub> ceramics could be obtained after pretreatment of the powder with hydrofluoric acid (HF), although the sample from the untreated powder was translucent. This powder treatment technique shows great promise for producing fine grained transparent Al<sub>2</sub>O<sub>3</sub> ceramics, using common-grade Al<sub>2</sub>O<sub>3</sub> powder.

## II. Experimental Procedure

A common-grade α-Al<sub>2</sub>O<sub>3</sub> powder (HFF5, Shanghai Wusong Chemical Co. Ltd., Shanghai, China) with a purity higher than 99.99% was used to prepare the transparent Al<sub>2</sub>O<sub>3</sub> ceramics. The powder was dispersed in 10 wt% HF to form a slurry with a solid load of 100 g/L; then, it was stirred for 6 h under continuous ultrasonication at room temperature. Afterwards, the powder was collected through filtering and cleaned by successive washing with distilled water for five times and ethanol alcohol for two times. The powder was dried at 100°C for 8 h, calcinated at 600°C in air for 1 h, and then spark plasma sintered (Dr. Sinter 1020, Sumitomo Coal Mining Co. Ltd., Tokyo, Japan) in a vacuum at a heating speed of 100°C/min. When the temperature increased to 700°C, a pressure of 80 MPa was applied, which remained constant during the later stage of sintering. The temperature was measured by an optical pyrometer focused on the half-through hole in the graphite die, and the variation of the total height of the graphite mold assembly with the temperature was recorded. After holding at the sintering temperature for 3 min, the applied pressure was removed and the power was turned off immediately, allowing the sample to cool naturally in the furnace. The final dimension of the sintered sample was 10 mm in diameter and 2.5 mm in thickness.

The surface layer of the sintered disk was removed (1 mm in depth) by deep grinding and mirror polished on both sides to a thickness of 0.5 mm, using 0.5 μm diamond paste. The microstructure was examined by scanning electron microscopy (SEM, Instrument JSM 6700F JEOL Ltd., Tokyo, Japan) on the polished surface thermally etched at 1150°C for 2 h. The in-line transmission was measured using a double-beam spectrophotometer (Model U-2800, Hitachi, Tokyo, Japan); the total forward transmission was measured using a PerkinElmer Lambda 950 (Perkin Elmer Inc., Waltham, MA) spectrophotometer equipped with an integrating sphere. The impurity level of the powder was analyzed using an inductively coupled plasma atomic emission spectrometer (Vista, Palo Alto, CA); the particle size distribution was analyzed (Zetaplus, Brookhaven) after the powder was ultrasonically dispersed in water for 6 h.

G. Wei—contributing editor

Manuscript No. 26691. Received August 13, 2009; approved November 9, 2009. This work was supported by the National Natural Science Foundation of China (50672112), the Key Project for Fundamental Research of Shanghai (09JC1415400), and the National Basic Research Program (2005CB623605).

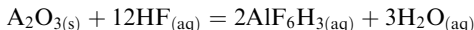
<sup>†</sup>Author to whom correspondence should be addressed. e-mail: liangaoc@online.sh.cn

### III. Results and Discussion

Chemical analysis indicates that the  $\text{Al}_2\text{O}_3$  powder is highly pure even before the treatment in HF; the only detectable impurities in it are Si (9 ppm), Fe (9 ppm), K (7 ppm), Na (6 ppm), and Ca (2 ppm). After the treatment in HF, the Si, K, and Na impurity contents decrease to 7, 1, and 4 ppm, respectively; while the content of Fe and Ca remain constant. It seems that the treatment of the powder in HF has not brought about any obvious change in its impurity level, probably because of the high purity of the original powder.

Figures 1(a) and (b) show the particle size distribution of the powders. The powder before treatment shows a bimodal particle size distribution, with two peaks centered at 360 and 1150 nm, respectively. After the treatment, the peak centered at 1150 nm is replaced with a small peak centered at 70 nm, while the peak centered at 360 nm was kept nearly unchanged. Figures 1(c) and (d) shows the SEM image of the untreated and pretreated  $\text{Al}_2\text{O}_3$  powders. In agreement with the result of the particle size distribution measurement, a clear reduction in aggregate size is observed after the powder treatment. For the untreated powder, large aggregates up to 1–1.5  $\mu\text{m}$  are frequently observed, while almost all the aggregates in the pretreated powder remain below 0.8  $\mu\text{m}$ . We believe that it is the disassociation of the aggregate that causes the reduction in aggregate size and the narrowed particle size distribution in the pretreated powder, as explained below.

When  $\text{Al}_2\text{O}_3$  powder is dispersed in aqueous HF solution, the  $\text{Al}_2\text{O}_3$  particles can be etched by HF according to the following reaction, which shows a negative Gibbs free energy change ( $\Delta G = -17$  kJ/mol)<sup>11,12</sup>:



This chemical etching is especially severe at the jointing point between the primary particles, due to its more disordered structure. Under the influence of an ultrasonic shock force and the chemical etching by HF, the joint points tend to become loose, leading to the disassociation of the aggregate and thereby a reduced aggregate size and narrowed particle size distribution in the pretreated powder. The reduction in aggregate size leads to a slight increase in the specific surface area of the powder from 4.7 to 5.2  $\text{m}^2/\text{g}$ .

Figure 2 shows the sintering behavior of the pretreated and untreated  $\text{Al}_2\text{O}_3$  powders, where the normalized displacement of the total height of the graphite mold assembly is used to approximate the real-time shrinkage during the densification process. It can be seen that both samples begin to shrink at about 900°C and the shrinkages increase abruptly above 950°C, reaching their maxima at about 1250° and 1300°C for the samples from the pretreated and untreated powder, respectively. A comparison between the two displacement curves finds that the pretreatment in HF has substantially enhanced the sinterability of the powder, which is mainly caused by the decrease in the aggregate size and probably the activation of the particle surface during the powder treatment process. The treatment of the powder in HF not only led to a decrease in the aggregate size as observed above, but also made the particle surface more activated due to the strong chemical etching effect of HF on the  $\text{Al}_2\text{O}_3$  particle surface. Both of the effects are helpful for sintering.

Density measurement indicates that the samples spark plasma sintered at 1200°–1400°C are all fully densified, independent of the powder treatment. Figure 3(a) shows the in-line transmission of the spark plasma sintered samples from the pretreated  $\text{Al}_2\text{O}_3$  powder. On the whole, the in-line transmission decreases with an increase in the sintering temperature due to the increase in light scattering caused by grain growth.<sup>3</sup> Taking the in-line transmission at the wavelength of 640 nm as an example,

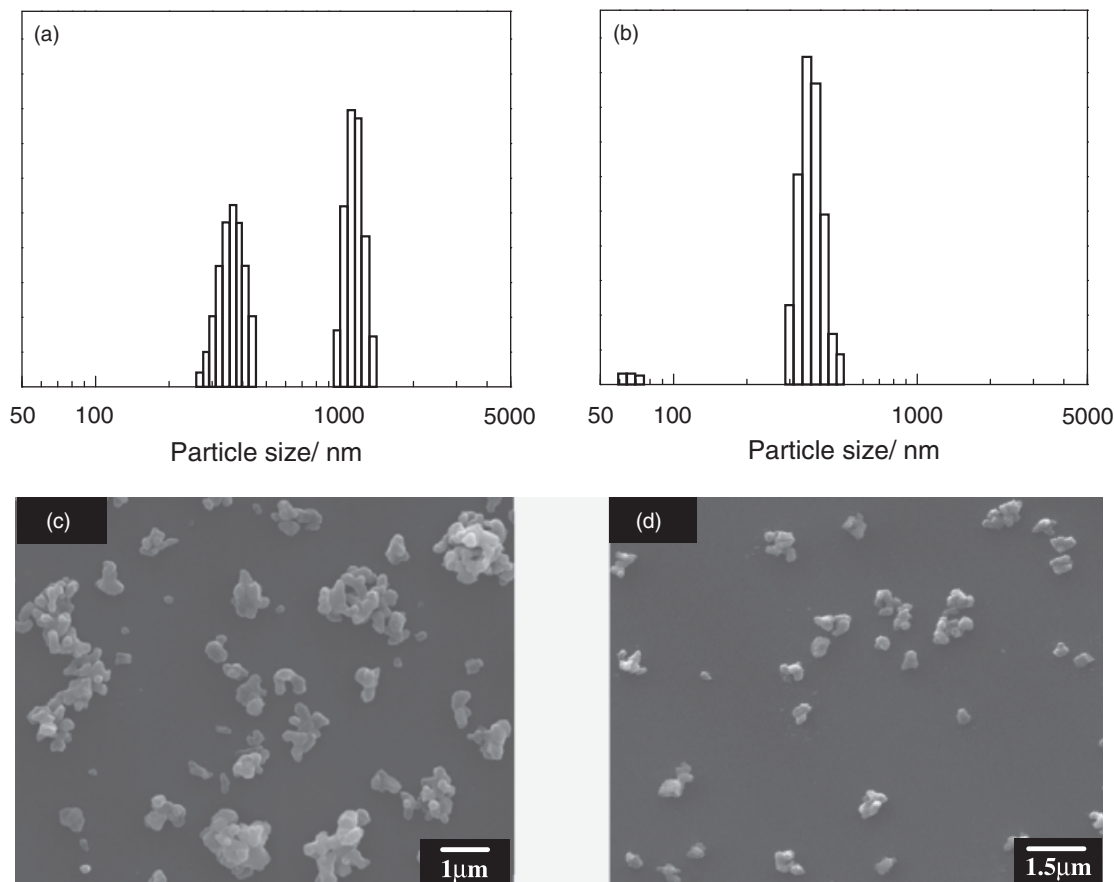


Fig. 1. Particle size distribution and scanning electron microscopy images of (a, c) untreated and (b, d) pretreated alumina powder.

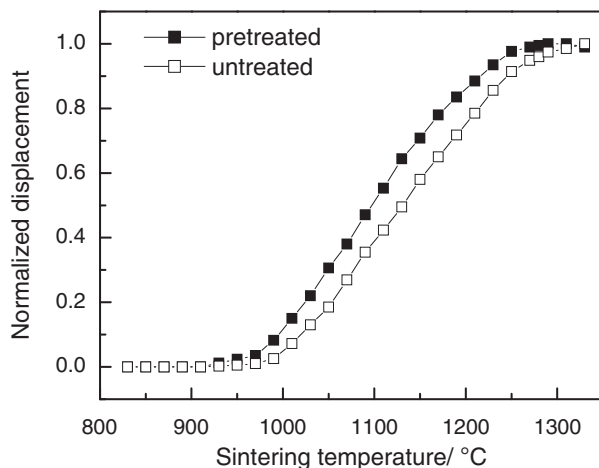


Fig. 2. Spark plasma sintering behaviors of the untreated and the pretreated alumina powders.

the samples sintered at 1300°, 1350°, and 1400°C show an in-line transmission of 0.53, 0.51, and 0.44, respectively. These in-line transmissions are much higher than that of the conventional transparent Al<sub>2</sub>O<sub>3</sub> ceramics, and are even comparable with the in-line transmission of some of the fine-grained transparent Al<sub>2</sub>O<sub>3</sub> reported before.

Using a highly sinterable Al<sub>2</sub>O<sub>3</sub> powder (TM-DAR, purity > 99.99%; Taimai Chemical Company Ltd., Nagano, Japan) as the raw material, fine-grained transparent Al<sub>2</sub>O<sub>3</sub> ceramics with grain sizes about 0.3 and 0.6 μm were prepared by Kim and Krell through spark plasma sintering and hot isostatic pressing, respectively.<sup>4,8</sup> These ceramics showed respective in-line trans-

mission of 0.33 and 0.64 at a sample thickness of 1.0 and 0.8 mm, and a wavelength of 640 nm. If their sample thickness are reduced to 0.5 mm as in the present work, the in-line transmission of 0.53 and 0.71 are expected according to the equation  $T_2 = (1-R)[T_1/(1-R)]^{d_2/d_1}$ , where  $T_1$  and  $T_2$  represent the in-line transmission at a sample thickness of  $d_1$  and  $d_2$ , and  $R = 0.14$ , is the reflection loss at the sample surfaces.<sup>4</sup> We can see that, the in-line transmission of the samples sintered at 1300°–1350°C from the pretreated Al<sub>2</sub>O<sub>3</sub> powder in the present work are obviously lower than that of the samples prepared by Krell, because of their larger grain size (1.8–2.2 μm), as will be revealed later; However, they are still nearly equivalent to that of the sample prepared by Kim, despite the much smaller grain size of the Kim's sample. The reason for the latter case is not clear, and most probably related with the difference in the sintering processes. Because of the slow heating rate (2°C/min) and prolonged holding time (20 min) at the sintering temperature, carbon contamination was relatively heavy in the sample prepared by Kim, which affected its transparency. While in comparison, carbon contamination should be much reduced in the present work, because of the fast heating rate (100°C/min) and short holding time (3 min) in sintering, as well as the relatively coarse powder used. Coarse powder with a small specific surface area can effectively depress the adsorption of the carbon species that is released from the graphite mold assembly, and thus reduces carbon contamination in the sintered sample. XPS measurement found no carbon in the sintered samples, probably due to the very low carbon content, which was below the detecting limit of the instrument (100 ppm). The low carbon contamination makes the samples in the present work show in-line transmission that are comparable with that of the sample prepared by Kim, although their grain sizes are much larger than the latter.

Figure 3(b) show the total forward transmission of the samples sintered at 1300° and 1350°C, which have the best transparency. In comparison with the in-line transmission, the total forward transmissions are much higher, especially at a low wave length range. This means that light scattering by grain boundaries and residual pores is still relatively significant in the samples. In fact, the gradual increase in both the total forward and in-line transmission with the wave length distinctively indicates the existence of light scattering within the samples. Especially the light scattering by residual pores, it has a strong influence on not only the in-line transmission but also the total forward transmission as well.<sup>8</sup>

Figure 4 shows the optical images of the spark plasma sintered samples from the untreated and pretreated Al<sub>2</sub>O<sub>3</sub> powders. Unevenness in the sample color, which is usually caused by heavy carbon contamination during spark plasma sintering,<sup>8</sup> is not observed for all these samples. The samples from the pretreated powder are highly transparent, and the underlying images immediately or 2.5 mm below the sample can be clearly seen, which is in good agreement with their high in-line transmission. As for the sample from the untreated powder, it is translucent at most. It is interesting that a pretreatment of the Al<sub>2</sub>O<sub>3</sub> powder in HF can lead to such a great improvement in the transparency of the sintered material.

As well known, light scattering caused by the birefringent Al<sub>2</sub>O<sub>3</sub> grains and residual pores are the two major factors affecting the transparency of high-purity Al<sub>2</sub>O<sub>3</sub> ceramics. Except for some special cases,<sup>2</sup> large grain size and high porosity usually lead to a strong light scattering and a serious deterioration of the material transparency. Figure 5(a) shows the SEM image of the sample that was spark plasma sintered at 1350°C from the untreated Al<sub>2</sub>O<sub>3</sub> powder. This sample possesses a coarse-grained microstructure with an average grain size of about 5.2 μm. Furthermore, owing to an exaggerated grain growth induced by the large aggregates in the starting powder and the entrapment of pores in the rapidly growing grains, large grains over 10 μm and intragranular pores larger than 100 nm are frequently observed in it. The resulting strong light scattering significantly reduces the transparency of the material, making it appear translucent.

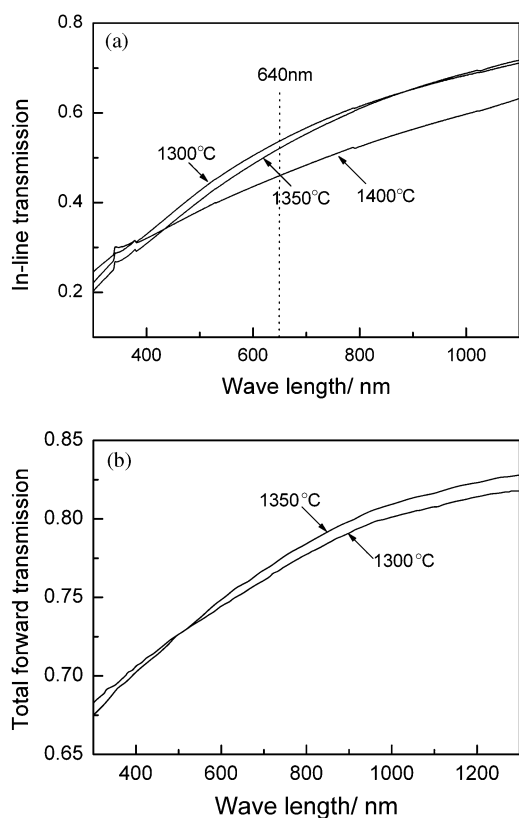
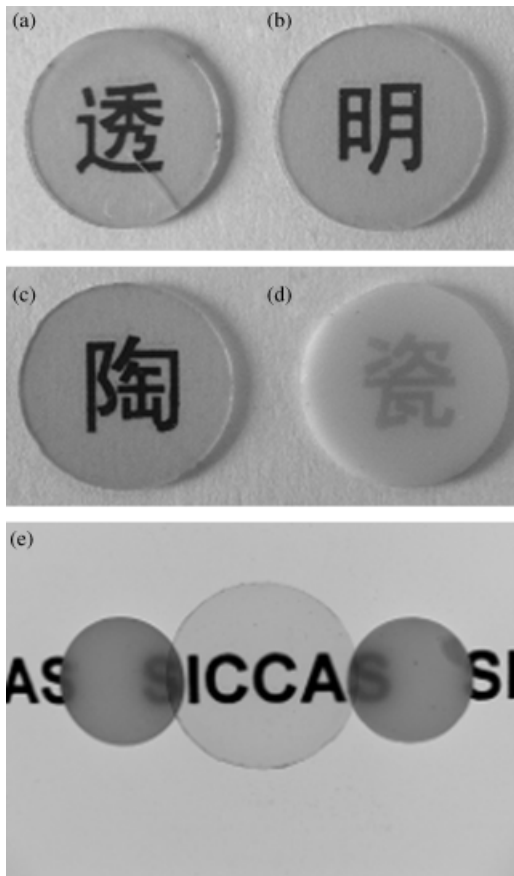


Fig. 3. (a) In-line transmission and (b) total forward transmission of the alumina ceramics that were spark plasma sintered at a different temperature from the pretreated powder. The shoulder at ~350 nm on the in-line transmission curve is a noise signal from the instrument.



**Fig. 4.** Optical images of the alumina ( $\text{Al}_2\text{O}_3$ ) ceramics that were spark plasma sintered at (a) 1250°C, (b) 1300°C, and (c–e) 1350°C, using (a–c) the pretreated and (d) the untreated  $\text{Al}_2\text{O}_3$  powder. All the samples are immediately on the text except sample (e), which is 2.5 mm above the text.

However, with respect to the samples from the pretreated powder, the results are quite different.

The pretreatment of  $\text{Al}_2\text{O}_3$  powder in HF not only reduces the aggregate size but also makes the remaining aggregates more liable to be disrupted under the mechanical and electric shock pressure during spark plasma sintering, because of the decreased aggregate strength caused by the powder treatment process. This significantly suppresses the abnormal grain growth induced by the large aggregates in the powder during sintering, leading to a remarkable improvement in the microstructure of the sintered materials. Figures 5(b) and (c) show the SEM images of the samples that were spark plasma sintered at 1300° and 1350°C from the pretreated  $\text{Al}_2\text{O}_3$  powder. These samples show relatively fine-grained microstructures with average grain sizes of 1.8 and 2.2  $\mu\text{m}$ , respectively. In comparison with the sample from the untreated powder shown in Fig. 5(a), the average grain sizes of these samples are reduced by more than one half, and the grain size distribution also becomes more uniform. What's more important, exaggerated grain growth and residual pores that are found in the sample from the untreated powder are scarcely observed here, although the gradual variation of light transmission with wave length implies that some residual pores may still present there. Such microstructure improvements effectively suppress light scattering, and cause a remarkable increase in the material transparency.

#### IV. Summary and Conclusions

In summary, the pretreatment of the  $\text{Al}_2\text{O}_3$  powder in HF led to a decrease in the aggregate size, and substantially improved

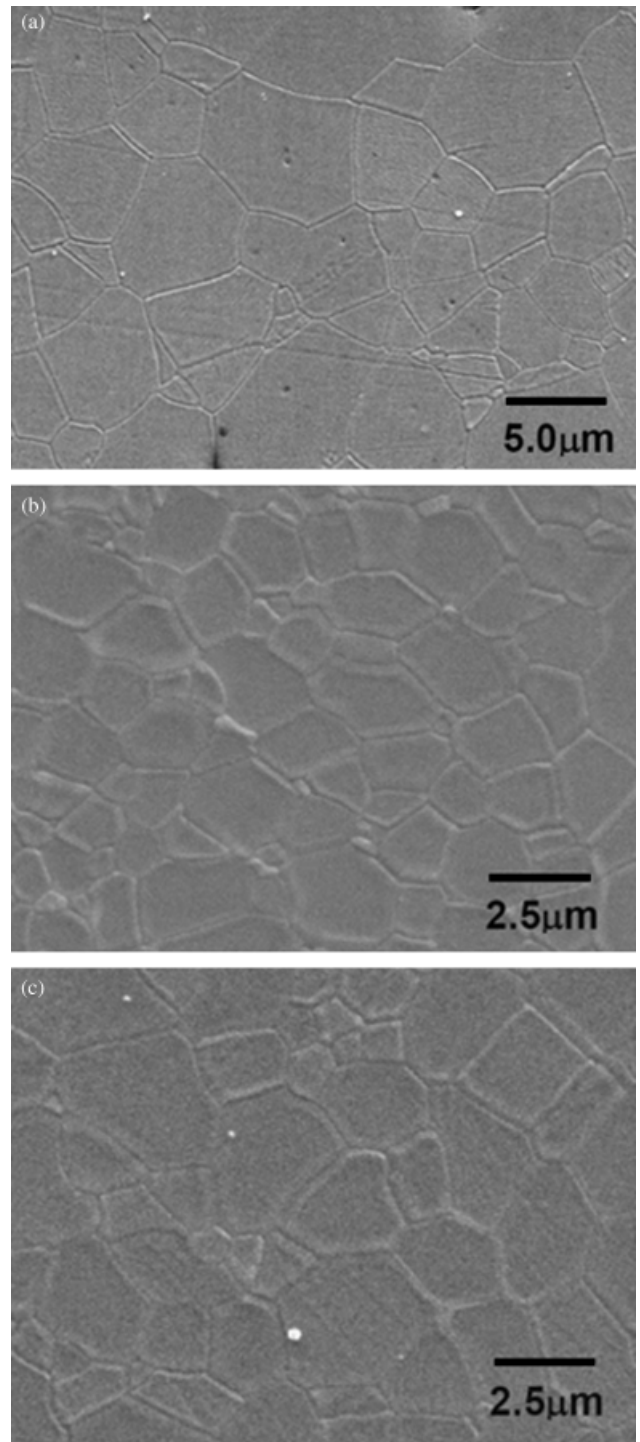


**Fig. 5.** Scanning electron microscopy images of the alumina ( $\text{Al}_2\text{O}_3$ ) ceramics that were spark plasma sintered at (a, c) 1350°C and (b) 1300°C, using (a) the untreated and (b, c) the pretreated  $\text{Al}_2\text{O}_3$  powder. The bright spots on image (a) and (c) are contaminant particles that fell on the sample surface during the thermal etching process.

the microstructure homogeneity and the optical property of the spark plasma sintered sample. In comparison with the sample sintered from the untreated powder, the samples sintered from the pretreated powder showed much more homogeneous microstructures with significantly reduced grain size and residual porosity. As a result, the transparency of the material was greatly improved, due to the suppression of light scattering. Highly transparent ceramics with an in-line transmission up to 0.53 at the visible light range were obtained, using the pretreated  $\text{Al}_2\text{O}_3$  powder.

## References

- <sup>1</sup>G. C. Wei and W. H. Rhodes, "Sintering of Translucent Alumina in a Nitrogen-Hydrogen Gas Atmosphere," *J. Am. Ceram. Soc.*, **83** [7] 1641-8 (2000).
- <sup>2</sup>X. J. Mao, S. W. Wang, S. Shimai, and J. K. Guo, "Transparent Polycrystalline Alumina Ceramics with Orientated Optical Axes," *J. Am. Ceram. Soc.*, **91** [10] 3431-3 (2008).
- <sup>3</sup>R. Apetz and M. P. B. Bruggen, "Transparent Alumina: A Light-Scattering Model," *J. Am. Ceram. Soc.*, **86** [3] 480-6 (2003).
- <sup>4</sup>A. Krell, P. Blank, H. Ma, T. Hutzler, M. P. B. Bruggen, and R. Apetz, "Transparent Sintered Corundum with High Hardness and Strength," *J. Am. Ceram. Soc.*, **86** [1] 12-8 (2003).
- <sup>5</sup>A. Krell and J. Klimke, "Effects of the Homogeneity of Particle Coordination on Solid-State Sintering of Transparent Alumina," *J. Am. Ceram. Soc.*, **89** [6] 1985-92 (2006).
- <sup>6</sup>D. T. Jiang, D. M. Hulbert, U. Ansilmi-Tamburini, T. Ng, D. Land, and A. K. Mukherjee, "Optically Transparent Polycrystalline  $Al_2O_3$  Produced by Spark Plasma Sintering," *J. Am. Ceram. Soc.*, **91** [1] 151-4 (2008).
- <sup>7</sup>B. Kim, K. Hiraga, K. Morita, and H. Yoshida, "Effect of Heating Rate on Microstructure and Transparency of Spark Plasma Sintered Alumina," *J. Eur. Ceram. Soc.*, **29** [2] 323-7 (2009).
- <sup>8</sup>B. Kim, K. Hiraga, K. Morita, H. Yoshida, T. Miyazaki, and Y. Kagawa, "Microstructure and Optical Properties of Transparent Alumina," *Acta Mater.*, **57** [5] 1319-26 (2009).
- <sup>9</sup>B. Kim, K. Hiraga, K. Morita, and H. Yoshida, "Spark Plasma Sintering of Transparent Alumina," *Scripta Mater.*, **57** [7] 607-10 (2007).
- <sup>10</sup>H. Mizuta, K. Oda, Y. Shibasaki, M. Maeda, M. Machida, and K. Ohshima, "Preparation of High-Strength and Translucent Alumina by Hot Iso-Static Pressing," *J. Am. Ceram. Soc.*, **75** [2] 469-73 (1992).
- <sup>11</sup>K. R. Mikeska and S. J. Bennison, "Corrosion of Alumina in Aqueous Hydrofluoric Acid," *J. Am. Ceram. Soc.*, **82** [12] 3561-6 (1999).
- <sup>12</sup>K. R. Mikeska, S. J. Bennison, and S. L. Grise, "Corrosion of Ceramics in Aqueous Hydrofluoric Acid," *J. Am. Ceram. Soc.*, **83** [5] 1160-4 (2000). □